

# Enzyme Catalysis: Beyond Classical Paradigms<sup>†</sup>

AMNON KOHEN AND JUDITH P. KLINMAN\*

Departments of Chemistry and Molecular and Cell Biology, University of California at Berkeley, Berkeley, California 94720

Received August 13, 1997

## Introduction

Despite many decades of intense study, a full description of enzyme catalysis at the molecular level remains to be achieved. A number of aspects of biocatalysis are widely accepted, including (i) the conversion of a chemical reaction from an inter- to an intramolecular process with the concomitant decrease in the entropy of activation and (ii) the stabilization of the transition state (TS) by the precise orientation of multiple functional groups at the enzyme active site. These functional groups perform the roles of general acid/base, electrophilic/nucleophilic catalysis and charge neutralization via electrostatic and H-bonding interactions. The process of covalent bond breaking and forming in enzyme catalysis is accompanied by substrate binding, product release, and protein rearrangement steps, which are rate determining for many enzymes. The resulting, multibarrier reaction path is sometimes very different from the noncatalyzed one and, by definition, has a lower free energy of activation ( $\Delta G^*$ ) (Figure 1).<sup>1</sup>

Transition-state theory (TST) is most commonly used in the description of protein catalysis. TST generally treats the reacting nucleus as a classical particle, vibrating in the reactant well zero-point energy (ZPE), that can be transferred to the product well ZPE along the electronic potential surface. The reaction rate is proportional to the Boltzmann distribution of energetic states between the reactant well and the transition state (TS), where the probability of product formation for particles with energy less than that of the TS is zero. This description has been generally accepted as a good approximation, with the important exception of electron-transfer reactions. In the latter case, Marcus theory describes a process whereby the electron is transferred solely by quantum-mechanical

Amnon Kohen received his B.Sc. degree in chemistry from the Hebrew University in Jerusalem in 1989, and his D.Sc. degree from the Technion-Israel Institute of Technology in 1994 on mechanistic studies of the reaction catalyzed by the enzyme Kdo8P synthase. He is currently a postdoctoral fellow in J. P. Klinman's group at the University of California at Berkeley, studying hydrogen tunneling and other features contributing to enzyme catalysis.

Judith P. Klinman is currently Chancellor's Professor in the Departments of Chemistry and Molecular and Cell Biology at the University of California, Berkeley. Her research is focused on nuclear tunneling in enzyme reactions, the mechanism of dioxygen activation in metal- and cofactor-containing enzymes, and the biogenesis and mechanism of quinoproteins.

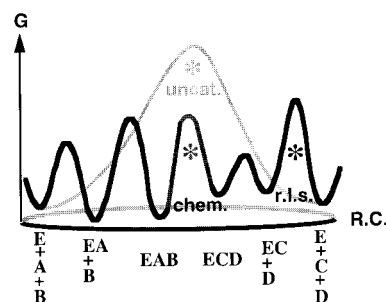


FIGURE 1. Free energy ( $G$ ) vs reaction coordinate ( $RC$ ) for an uncatalyzed  $A + B \rightarrow C + D$  reaction (gray) and an enzyme ( $E$ )-catalyzed one (black). The uncatalyzed TS and the chemical and rate-limiting TS for the enzymatic reaction are denoted by an asterisk.

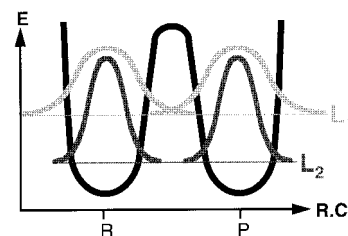
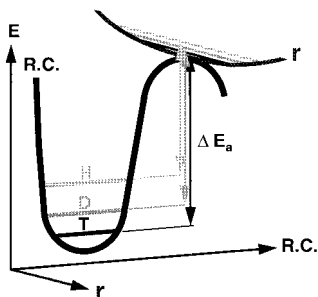


FIGURE 2. An example of ground-state nuclear tunneling along the reaction coordinate ( $RC$ ). The reactant well ( $R$ ) is on the left side and product well ( $P$ ) on the right. The light and dark lines describe a light ( $L_1$ ) and a heavy ( $L_2$ ) isotope probability function, respectively. The greater the overlap of the  $R$  and  $P$  probability functions, the higher is the tunneling probability.

tunneling.<sup>2</sup> The rearrangement of the enzyme active site from a reactant to a product state determines the activation energy and reaction rate. The phenomenon of a particle tunneling through a barrier results from the wave/particle duality of matter and occurs when the probability of finding a particle “under” a barrier at the reactant site overlaps with the probability of finding it “under” the barrier at the product site (Figure 2).

Can tunneling of particles heavier than the electron contribute to their rate of transfer in biological systems? Let us examine another quantum mechanical property of free particles, their de Broglie wavelength ( $\lambda = h/(2mE)^{1/2}$ ). This wavelength is 18 Å for an electron with an energy of 10 kJ/mol. Calculation of the de Broglie wavelength for a hydrogen with similar energy yields 0.5 Å for <sup>1</sup>H (protium, H), 0.31 Å for <sup>2</sup>H (deuterium, D), and 0.25 Å for <sup>3</sup>H (tritium T). Note that, in the case of particles bound in the ground state, i.e., the C–H bond, the transferred nucleus is formally undergoing a translation from donor to acceptor atoms at the TS. A key feature in evaluating quantum behavior is the relationship of a particle's wavelength to the barrier width it must traverse. In the case of hydrogen,  $\lambda$  is in the range of transfer distances anticipated for many biological processes. Apparently, looking for quantum-mechanical tunneling in biological hydrogen-transfer processes deserves a serious examination.

<sup>†</sup> This Account is dedicated to my teachers, Edward Thornton and Irwin Rose, for sharing their deep understanding and appreciation of isotope and enzyme chemistry.



**FIGURE 3.** Different energies of activation ( $\Delta E_a$ ) for H (light gray), D (gray), and T (dark gray) resulting from their different zero-point energies (ZPE) at the ground state (GS) and transition state (TS). The GS-ZPE is constituted by all degrees of freedom but mostly the ZPE stretching frequency, and the TS-ZPE is constituted by all degrees of freedom orthogonal to the reaction coordinate ( $r$ ). This type of consideration (quantum mechanical ZPE with no tunneling) is depicted as semiclassical. Such a model predicts KIE for isotopes 1 and 2 according to  $\ln(k_1/k_2) = (\Delta E_{a2} - \Delta E_{a1})/RT$ .

Exploring the importance of hydrogen tunneling in enzyme catalysis is the subject of this Account. After a general presentation of the utility of isotope effects (IEs) to explore tunneling, experimental examples which suggest a general role of proton, hydrogen atom, and hydride tunneling under physiological conditions will be presented. As the interpretation of the experimental results is highly dependent upon theoretical models, different models will be presented and examined. For small molecular systems, both modeling of reaction dynamics and experimental observations suggest that hydrogen tunneling only becomes significant at temperatures too low to be of biological importance. Is it possible that the environment of enzyme active sites enhances the probability of tunneling at physiological temperatures? Does such a phenomenon contribute to their rate enhancement? The mutual relationships between experiments and theory will be discussed, together with their impact on our understanding of enzyme catalysis.

## Kinetic Isotope Effects (KIEs)

KIEs of hydrogen are relatively large due to the large mass ratio between H, D, and T, and can serve as a good probe for exploring nonclassical behavior. Classical, semiclassical, and quantum mechanical models each predict different outcomes with regard to the magnitude of the isotope effects, their mutual relationships, and their temperature dependences. Classically, only very small KIEs are predicted from the nuclear mass dependence of the potential surface. Semiclassically, the magnitude of KIEs arises from differences in the zero-point energy levels of the isotopes (Figure 3).<sup>3,4</sup> The exponential relationship between the protium-to-tritium (H/T) KIE and deuterium-to-tritium (D/T) KIE within this model is predicted to be  $\ln(\text{H/T})/\ln(\text{D/T}) = 3.3$ .<sup>5</sup> In a TST-like model with a tunneling correction,<sup>3</sup> the lighter isotope tunnels at lower energy under the barrier (Figure 4), and the relationship  $\ln(\text{H/T})/\ln(\text{D/T})$  increases to values significantly larger than 3.3.<sup>5</sup> In the case of extensive tunneling, a range of values is possible.<sup>6</sup>

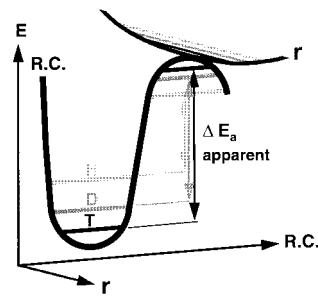


**FIGURE 4.** Tunneling correction for a TST type of model. The color code and coordinates are as in Figure 3. In addition to its higher ZPE, the lighter isotope tunnels at a lower energy under the top of the barrier, resulting in smaller  $\Delta E_a$  (relative to that of the heavier isotope) than in the semiclassical model (Figure 3).

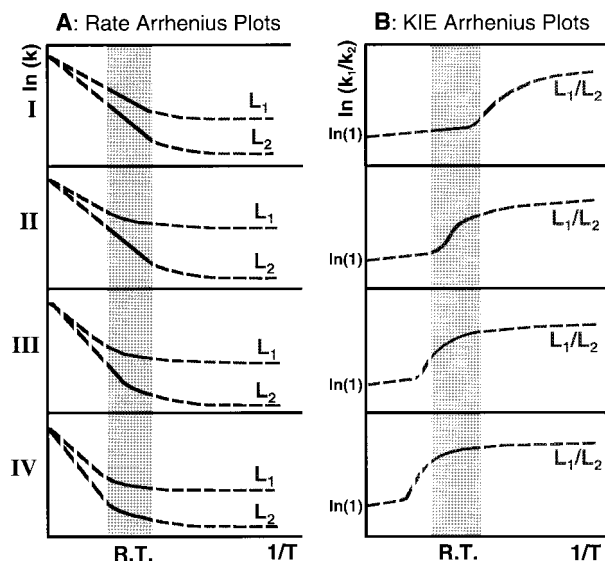


**FIGURE 5.** (A) Arrhenius plot of  $\ln(\text{rate})$  versus reciprocal absolute temperature ( $1/T$ ), for a light isotope ( $L_1$ ) and a heavier isotope ( $L_2$ ). (B) Arrhenius plot of  $\ln(k_1/k_2)$  versus  $1/T$ . The experimental temperature range is highlighted by gray. The  $L_1/L_2$  KIE on the Arrhenius preexponential factors ( $A_1/A_2$ ) is the intercept of the tangent to the curve at the experimental temperature range. Four experimental systems (I–IV) which exhibit different  $A_1/A_2$  values, associated with different degrees of tunneling, are presented. System I: no tunneling contribution; results in an  $A_1/A_2$  of unity. System II: some tunneling contribution to the  $L_1$  reaction whose plot curves up; results in  $A_1/A_2 < 1$ . System III: some tunneling contribution to  $L_2$  and  $L_1$ ; can produce  $A_1/A_2$  close to unity (as for system I). System IV: both isotopes tunnel significantly with similar  $\Delta E_a$  values; gives  $A_1/A_2 > 1$ .

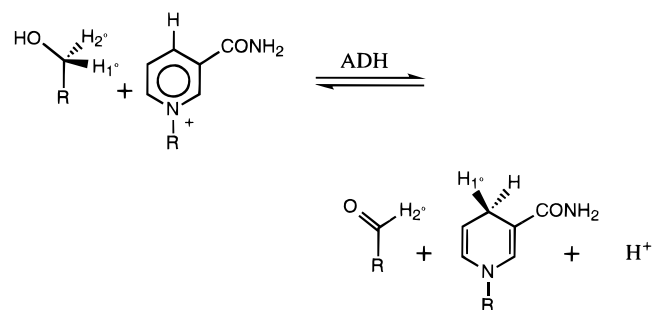
Another indication for tunneling may come from the temperature dependence of KIEs. Plotting  $\ln(k)$  vs the reciprocal of temperature ( $1/T$ ) for two isotopes ( $L_1$  and  $L_2$ , Figure 5A) shows the expected decrease in slope as tunneling becomes more dominant at low temperatures. Eventually, Arrhenius plots are expected to plateau (due to the presence of quantum effects), but this plateau occurs at a higher temperature for the lighter isotope(s) (cf. Figure 5, refs 7 and 8 and discussions below). As a consequence, a plot of  $\ln(L_1/L_2)$  vs  $1/T$  gives the result shown in Figure 5B, where the slope ( $(\Delta E_{a(L2)} - \Delta E_{a(L1)})/R$ ) and the intercept (the isotope effect on the Arrhenius preexponential factor,  $A_{\text{H or D}}/A_{\text{T}}$ ) are changing. In the

limit of high temperature, as well as in models which do not allow tunneling, the KIE on the Arrhenius preexponential factor is expected to be very close to unity.<sup>3,4</sup> Different degrees of tunneling will result in different IEs on Arrhenius preexponential factors, which may be either reduced or amplified relative to the high-temperature limit.

Throughout the studies of tunneling from this laboratory, both the exponential relationship between multiple KIEs and the temperature dependence of KIEs have been investigated in an attempt to observe possible deviations from semiclassical predictions. Thus far, all studies have focused on C–H bond cleavage processes, since hydrogen isotopes can be stably incorporated at carbon centers. Although tunneling is likely to be prevalent in hydrogen transfers between oxygen and nitrogen atoms, experimental systems have not yet been designed for the measurement of these effects.

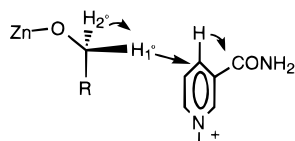
## Alcohol Dehydrogenases (ADH)

Alcohol dehydrogenase (ADH) catalyzes hydride transfer from substrate to the C4 carbon of the nicotinamide ring of NAD<sup>+</sup>, to produce the corresponding aldehyde:



In the early 1980s, anomalously large secondary KIEs were observed in both yeast and horse liver ADH-catalyzed reaction.<sup>9</sup> These KIEs could not be explained by semiclassical mechanics, but were consistent with a quantum mechanical correction incorporated into a TST-like model.<sup>10</sup>

Studies of yeast ADH (YADH) showed that the hydrogen-transfer step is mostly rate limiting. Competitive KIEs measured for this enzyme at 25 °C with isotopically labeled benzyl alcohols resulted in exponents of  $3.58 \pm 0.09$  and  $10.2 \pm 2.4$  for primary and secondary KIEs, respectively.<sup>9</sup> The upper semiclassical limit for these exponents, calculated from reduced masses without coupled motion, is 3.3; therefore, these results provided experimental support for the proposal that *both* coupled motion and tunneling contribute to hydride transfer in ADH. Coupled motion refers to a case where both primary and secondary hydrogen motions contribute to the reaction coordinate:



In this way, tunneling is reflected in both the primary and secondary hydrogens of the substrate. The much larger breakdown of the exponent for the secondary isotope is a consequence of the fact that secondary isotope effects are generally small (close to 1), and does not imply that the nontransferred position is tunneling more than the primary hydrogen. It is important to note that exponential relationships lower than 3.3 can be a result of either extensive tunneling<sup>6</sup> or simply (and commonly) of the isotopically sensitive step not being fully rate limiting. For example, if the H transfer is fast relative to binding steps (low chemical barrier in Figure 1), an H/T KIE lower than its intrinsic value is observed,<sup>11</sup> decreasing the observed exponent (a phenomenon called “kinetic complexity”). However, exponents the size seen with YADH ( $10.2 \pm 2.4$ ) can only (thus far) be satisfied by invoking hydrogen tunneling.<sup>4,12</sup> Later experiments with YADH, using para-substituted benzyl alcohols, revealed that the above effect with unsubstituted benzyl alcohols is also found for substituted benzyl alcohols with altered internal thermodynamics.<sup>13</sup>

Studies of horse liver ADH (HLADH) were more challenging as the reaction rate is partially limited by the release of the products.<sup>14</sup> This kinetic complexity partly “masks” the observed KIE, which at 25 °C did not clearly support hydrogen tunneling. The crystal structure of the enzyme was used to design site-directed mutants with enhanced rates of substrate/product release. By changing a residue in the active site that is in van der Waals contact with the alcohol to one with a larger side chain (Leu<sup>57</sup> → Phe or Phe<sup>93</sup> → Trp), hydrogen tunneling was demonstrated in a fashion similar to that of YADH. For the Phe<sup>93</sup> → Trp mutant, the temperature dependence of the primary KIE was determined, indicating values for  $A_H/A_T$  and  $A_D/A_T$  lower than predicted from semiclassical models.<sup>12</sup> As illustrated in Figure 5, system II, low preexponential factors may result from a moderate tunneling contribution that is more significant for the lighter isotope. The overall picture for HLADH suggests that the wild-type enzyme is characterized by significant tunneling, but that this is obscured by a slow release of product when a protiated substrate is used.

In a new series of active site mutants recently examined, the size of a side chain on the back (nonreacting) side of the nicotinamide ring of the cofactor was changed (Val<sup>203</sup> → Leu, Ala, and Gly) with and without the mutation in the alcohol binding pocket (Phe<sup>93</sup> → Trp).<sup>15</sup> Initial velocity and KIE measurements with these mutants suggest a correlation between their catalytic efficiency ( $V/K$ ) and the extent of tunneling contribution, as indicated by the exponents describing secondary KIEs (Figure 6). This result suggests that hydrogen tunneling may be directly related to an increase in the catalytic efficiency of an enzyme. The crystal structures of two of these mutants (Phe<sup>93</sup> → Trp and Val<sup>203</sup> → Ala) having high and low tunneling contributions, respectively, showed that the low tunneling mutant (Val<sup>203</sup> → Ala) binds the nicotinamide ring in such a manner that it is rotated an average of 10° and ~0.8 Å away from the alcoholic carbon. This is the

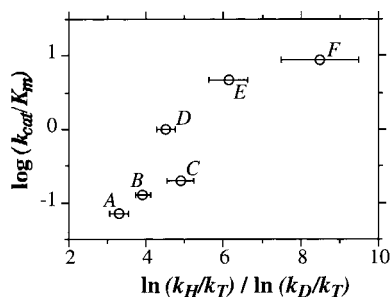


**FIGURE 6.** Correlation of  $\log(k_{\text{cat}}/K_m)$  and  $\ln(k_{\text{H}}/k_{\text{T}})/\ln(k_{\text{D}}/k_{\text{T}})$  for the secondary KIE with site-directed mutants of alcohol dehydrogenase: (A) Val<sup>203</sup> → Gly, B: Val<sup>203</sup> → Ala:Phe<sup>93</sup> → Trp, C: Val<sup>203</sup> → Ala, D: Val<sup>203</sup> → Leu, E: Phe<sup>93</sup> → Trp, F: Leu<sup>57</sup> → Phe. Tunneling is indicated when the ratio of  $\ln(k_{\text{H}}/k_{\text{T}})$  to  $\ln(k_{\text{D}}/k_{\text{T}})$  is >3.3 (see the text).

first evidence connecting the hydrogen-transfer distance in an enzyme reaction with the degree of tunneling and catalytic efficiency.<sup>15</sup>

Recent studies of a thermophilic ADH from *Bacillus stearothermophilus* with benzyl alcohol at 65 °C resulted in secondary H/T and D/T KIEs that are related by an exponent of  $15 \pm 5$ .<sup>16</sup> This result, suggesting that tunneling is still significant at 65 °C, leads to some general conclusions. As mentioned above (Figure 5A), a reduced tunneling contribution is expected at elevated temperature. Yet, the active site of the thermophilic enzyme at 60–70 °C appears similar to that of the mesophilic enzyme at 25 °C. Since tunneling is expected to have specific geometric and dynamic requirements (see below), this implies conserved behavior for enzymes evolved to work at different temperatures.

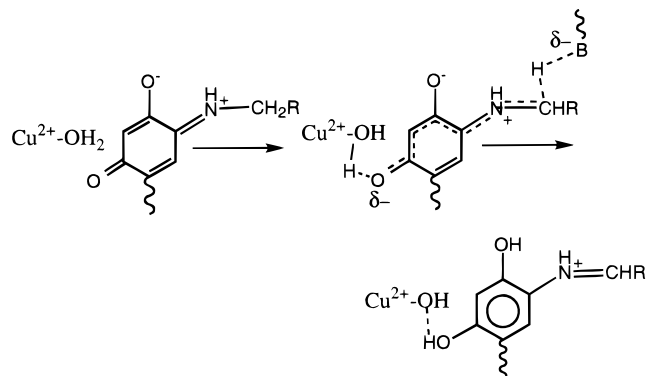
A number of theoretical models have been developed to try to explain the behavior of ADH and related systems. Of particular interest are the works of Truhlar<sup>17</sup> and Kreevoy<sup>7</sup> where hydride transfer was found to involve a significant tunneling contribution as a corner-cutting process, ~4–8 kJ/mol beneath the top of the reaction barrier. Kim and Kreevoy, using variational TST with a large tunneling correction, presented results (their Figure 3)<sup>7</sup> which are in excellent agreement with our Figure 5. These works conclude that deuterium tunnels from a more classical configuration than protium, i.e., nearer the top of the conventional barrier. The protium smaller mass allows the barrier to be penetrated at a wider point and lower energy.

## Amine Oxidases (AO)

Amine oxidases catalyze the oxidative deamination of primary amines to the corresponding aldehydes:  $\text{RCH}_2\text{-NH}_3^+ + \text{O}_2 + \text{H}_2\text{O} \rightarrow \text{RCHO} + \text{H}_2\text{O}_2 + \text{NH}_4^+$ . Unlike ADHs, where hydride transfer is involved, the AO-catalyzed reactions proceed through proton or net hydrogen atom abstraction. Two AOs have been examined, and both exhibit protium and deuterium tunneling.

Bovine serum AO (BSAO) is a copper-containing enzyme with a trihydroxyphenylalanine quinone (TPQ) cofactor. The mechanism proposed for its reductive half-reaction, as presented below, involves the conversion of

a substrate to a product Schiff base complex via an active site base-catalyzed proton abstraction:<sup>18</sup>



The first data suggestive of proton tunneling in this system came from a very large primary KIE which exceeded the semiclassical limit.<sup>19</sup> Later, a systematic investigation of primary and secondary H/T and D/T KIEs in the range of 0–45 °C was performed. The primary H/T and D/T KIEs increased from 25.4 and 2.8, respectively, at 45 °C, to 59.1 and 3.7, respectively, at 0 °C.<sup>20</sup> While such large KIEs can be highly suggestive of hydrogen tunneling,<sup>3</sup> they do not constitute proof of tunneling. In this case, more direct evidence came from the magnitude of H/T and D/T IEs on the Arrhenius preexponential factors. The calculated semiclassical limits are  $A_{\text{H}}/A_{\text{T}} > 0.6$  and  $A_{\text{D}}/A_{\text{T}} > 0.9$ <sup>21</sup> compared to measured values of  $A_{\text{H}}/A_{\text{T}} = 0.12 \pm 0.04$  and  $A_{\text{D}}/A_{\text{T}} = 0.51 \pm 0.10$ . Furthermore, the measured  $\Delta E_{\text{a(T)}} - \Delta E_{\text{a(H or D)}}$  values for the primary KIE were 14 and 4.5 kJ/mol for H/T and D/T, respectively; the upper semiclassical limit for these values is 8.3 and 2.5 kJ/mol, respectively.

Two models could have explained the BSAO results without invoking tunneling. Elevated KIEs can result from branched reaction mechanisms that lead to two or more products via a common intermediate.<sup>22</sup> This possibility has been ruled out for BSAO, because all evidence indicates a single product (either reduced cofactor from stopped-flow experiments or aldehyde from steady-state measurements). Anomalous isotope effects on the Arrhenius prefactors can also result from increased kinetic complexity at higher temperature, suppressing the KIE at high temperature relative to low temperature (imposing an artificially large slope and a low intercept in the  $\ln(\text{KIE})$  vs  $1/T$  Arrhenius plot).<sup>23</sup> This second possibility was tested by stopped-flow H/D KIE measurements which showed good agreement with the steady-state experiments over a wide temperature range, supporting a single rate-limiting step and ruling out kinetic complexity for H as well as D and T.

In contrast to the ADHs, no abnormalities were observed for secondary KIEs, indicating little or no coupled motion along the reaction coordinate. Furthermore, for BSAO, the exponents relating primary KIEs were within experimental error of the semiclassical value (~3.3) at all temperatures. A major question must now be considered: why is it that while the preexponential Arrhenius

factors give compelling evidence for tunneling of both protium and deuterium, no abnormalities were found on the exponents relating primary KIEs? First, as demonstrated by Saunders,<sup>5</sup> the breakdown of these exponents becomes very difficult to detect when isotope effects are large. Second, simulation of a Bell-like tunneling correction ( $Q_{\text{H or D}}/Q_{\text{T}}$ ) to TST calculations showed that while these exponents exceed the 3.3 value for moderate tunneling, extensive tunneling could lead to values  $\leq 3.3$  for BSAO.<sup>6</sup> Since a significant extent of deuterium tunneling is suggested by the low  $A_{\text{D}}/A_{\text{T}}$ , such a possibility seems to be reasonable. Huskey<sup>10</sup> has also pointed out the major role of coupled motion in the manifestation of abnormal exponents for tunneling systems. All of the above data are in accordance with BSAO having system II (Figure 5) behavior for both H and D ( $L_1 = \text{H or D}$ ;  $L_2 = \text{T}$ ).

Another AO which was examined is bovine liver monoamine oxidase B (MAO-B). This is a flavoenzyme (FAD cofactor), whose catalytic mechanism may involve proton or direct hydrogen atom transfer.<sup>24</sup> Competitive KIEs with *p*-methoxybenzylamine as the substrate were measured. A small, temperature-independent kinetic complexity was shown to have only a minor effect on the Arrhenius prefactor IEs. The  $A_{\text{H}}/A_{\text{T}}$  and  $A_{\text{D}}/A_{\text{T}}$  were  $0.13 \pm 0.03$  and  $0.52 \pm 0.05$ , respectively, which are again well below the semiclassical lower limit.<sup>24</sup> The secondary H/T KIEs were rather large, 1.26 at 43 °C and 1.39 at 10 °C, but generally this enzyme gave a signature of protium and deuterium tunneling similar to that of BSAO. This suggests that although BSAO and MAO-B have very different redox mechanisms, both utilize similar physical features to catalyze hydrogen transfer.

Some theoretical methods were developed in an attempt to explain and model the BSAO results. Bruno and Bialek<sup>25</sup> presented a theory in which hydrogen tunneling is mediated by classical thermal fluctuations of the enzyme. Harmonic oscillation of the barrier controlled the transfer rate by shortening the tunneling distance. Their expression for vibrationally enhanced tunneling fit the BSAO data as well as the original linear Arrhenius fitting. A different approach has been proposed by Antoniou and Schwartz,<sup>26</sup> who have developed tunneling models consisting of a fluctuating double-well system. In the first model, the original approach of Borgis–Hynes<sup>27</sup> has been modified to allow for a wider range of vibrational frequencies of the protein. With only ground-state hydrogen tunneling, the KIE temperature dependence is caused by a thermally excited protein mode that modulates the barrier width and shape (coordinate **q** in Figure 7). The wave functions' coherency (enabling tunneling) is destroyed by active site dynamics which alter the double-well system, thereby trapping the product in the product well (coordinate **p** in Figure 7). Note that when the particle tunnels back and forth across a barrier, no reaction rate results unless this coherence is removed and the particle becomes trapped in the product well. Such a process is commonly depicted as dissipative tunneling. In the second model of Antoniou and Schwartz, over the barrier transfer and tunneling from excited states were

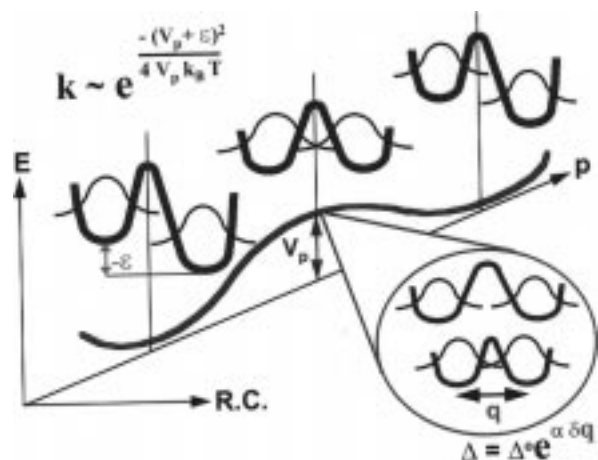
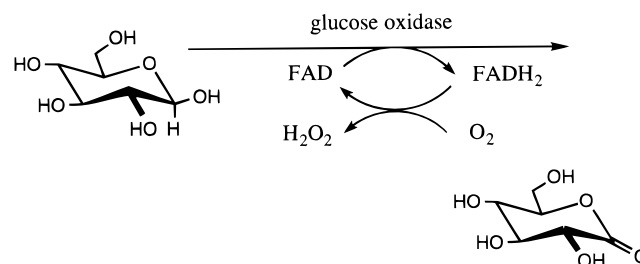


**FIGURE 7.** Marcus-like model<sup>26,27</sup> of ground-state hydrogen tunneling. Coordinate **p** describes the energy profile (green) of the environment dynamics, which changes the symmetry of the reaction coordinate (RC) double-well system (brown), enabling dissipative tunneling (see the text). The probability functions are shown in blue. The upper equation shows that the temperature dependence of the reaction rate,  $k$ , is a function of  $V_p$ , the barrier height along the **p** coordinate, and  $\epsilon$ , the exothermicity of the reaction ( $k_B$  is Boltzmann's coefficient). This term is common to electron and proton tunneling, and is isotope independent. The temperature dependence of KIEs is caused by thermally excited environmental (active site) modes that modulate the barrier shape. As demonstrated by the magnified region, the distance **q** between the reactant and product wells fluctuates, changing the tunneling probability ("tunneling splitting",  $\Delta$ ).  $\Delta^0$  is  $\Delta$  at distance  $q^0$  ( $T = 0$ ), and  $\alpha$  is the proportionality coefficient which is isotope dependent (cf. the lower equation). Notably, the temperature dependence of neither  $k$  nor KIE is a function of the reaction barrier height.

incorporated. Although their two models predict very different KIE temperature dependences, they both fit the currently available BSAO results.

## Glucose Oxidase (GO)

Glucose oxidase catalyzes the oxidation of glucose to  $\delta$ -gluconolactone and the subsequent reduction of oxygen to hydrogen peroxide:



The enzyme contains one FAD cofactor per monomer and is a homodimer with a molecular weight of 132 000–320 000, depending on the extent of surface glycosylation. In the reductive half-reaction, the anomeric hydrogen is likely to undergo hydride transfer to the FAD-N5 position, although an alternative mechanism involving proton transfer from the substrate cannot be excluded.<sup>28</sup>

Steady-state and pre-steady-state kinetic investigations of GO<sup>29</sup> indicated partial rate limitation by glucose binding

but less so for binding of 2-deoxyglucose. This led to the choice of 2-deoxyglucose for detailed studies of the chemical step. An important feature of this system is that there is no secondary hydrogen to complicate the interpretation of results. Three GO glycoforms were investigated for possible hydrogen tunneling.<sup>30</sup> These glycoforms have identical polypeptide chains with five glycosylation sites on the protein surface, but have differently sized polysaccharide chains. The degree of glycosylation was controlled either by deglycosylating the enzyme or by producing a highly glycosylated form by expression in yeast.<sup>31</sup> Among the glycoforms characterized, the lightest one had only eight sugars (MW of 136 000), the next about 120 sugars (MW  $\approx$ 155 000), and the heaviest about 400 sugars (MW  $\approx$ 205 000). Initial velocity studies with glucose, for which binding is rate limiting,<sup>30</sup> suggest that the deeply buried active site and enzyme itself are not deformed by glycosylation.

Competitive KIEs were measured over a temperature range of 0–45 °C with labeled 2-deoxyglucose. The exponents relating primary KIEs were all lower than 3.3 (2.83–2.97), indicating that some kinetic complexity is suppressing the H/T KIE. The D/T KIEs, on the other hand, appear to be fully expressed. Isotope effects on Arrhenius prefactors, determined from the relationship between  $\ln k_D/k_T$  and  $1/T$  were  $0.89 \pm 0.04$ ,  $1.30 \pm 0.10$ , and  $1.47 \pm 0.09$  for the MW 203 000, 155 000, and 136 000 glycoforms, respectively. The value measured for the lightest glycoform is significantly above the semiclassical range for  $A_D/A_T$  of 0.9–1.22,<sup>3,4,21</sup> as predicted in the case where both deuterium and tritium tunnel. The fact that the highest  $A_D/A_T$  occurs with the lightest glycoform suggests that all three glycoforms support deuterium tunneling, but that only the MW 136 000 glycoform permits significant tritium tunneling as well. The data for GO can be interpreted in the context of Figure 5, with the behavior of the MW 203 000 form characteristic of region II, while the lightest glycoform is in region IV. This trend in behavior with protein glycosylation led to the prediction of a correlation between  $A_D/A_T$  and the enthalpy of activation for H-transfer. Indeed, when [1-<sup>2</sup>H]-2-deoxyglucose was used as substrate (whose H-transfer is rate limiting), the enthalpy of activation for the MW 205 000, 155 000, and 136 000 forms was found to decrease from  $13.7 \pm 0.3$  to  $11.0 \pm 0.3$  and  $8.1 \pm 0.4$  kcal/mol as the magnitude of  $A_D/A_T$  (and hence tunneling) increased (Figure 8).

These results indicate that the degree of hydrogen tunneling with glucose oxidase varies with the extent of protein glycosylation, such that tunneling is greatest with the least glycosylated protein. These findings suggest a link between modification of the protein envelope (>22 Å away from the active site) and the nature of hydrogen tunneling during catalysis in the active site. The origin of these differences may reside in different degrees of protein dynamical motion among the three glycoforms of GO, as glycosylation can induce protein rigidity.<sup>32</sup> As discussed above and below, dynamic fluctuations are required in most modern models for hydrogen tunneling.

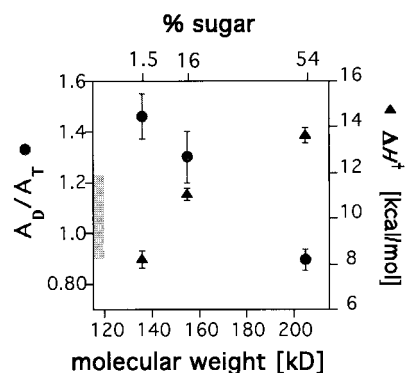
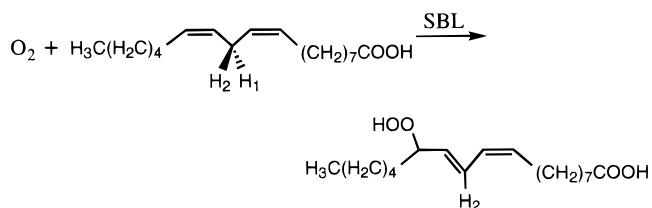


**FIGURE 8.** Relationship between the KIE on the Arrhenius preexponential factors  $A_D/A_T$  (circles) and enthalpies of activation for [1-<sup>2</sup>H]-2-deoxyglucose (triangles) as a function of the degree of glycosylation of glucose oxidase. The semiclassical calculated range for  $A_D/A_T$  is 0.9–1.22 (as highlighted by gray bar).

## Lipoxygenase

Soybean lipoxygenase-1 (SBL) catalyzes hydroperoxidation of linoleic acid (LA) to 13(*S*)-hydroperoxy-9(*Z*),11(*E*)-octadecadienoic acid (LOOH):



The precise chemical mechanism of SBL is a subject of some controversy.<sup>33,34</sup> It was proposed that a hydrogen atom is abstracted from the C11 position of the substrate to yield a delocalized organic radical which then reacts with dioxygen, producing a peroxy radical.<sup>35</sup> The hydrogen radical is likely to reduce the enzyme  $\text{Fe}^{3+}-\text{OH}$  to  $\text{Fe}^{2+}-\text{H}_2\text{O}$ . The hydrogen transfer was shown to be the rate-limiting step of the reaction at temperatures above 32 °C.<sup>8,36</sup> Competitive and noncompetitive KIE measurements under steady-state and pre-steady-state conditions demonstrate a H/D KIE of about 55 above 32 °C.<sup>8,36–38</sup> Such a KIE is much larger than predicted by semiclassical calculation.<sup>3</sup> Some explanations for this KIE, such as magnetic spin effects<sup>38</sup> or branching of isotopically sensitive steps,<sup>8,36</sup> have been ruled out, leaving tunneling as the most reasonable explanation. As discussed for BSAO, large KIEs are not sufficient evidence for tunneling; however, additional compelling evidence does exist for SBL. The observed enthalpies of activation for protonated and deuterated substrates were similar and low (1.5–3.4 kcal/mol), leading to  $A_H/A_D$  in the range of 12–60, which is clearly above the semiclassical limit of 1.22. As suggested by Jonsson et al.,<sup>8</sup> this can be understood in the context of Figure 5, system IV. Table 1 places the behavior of SBL in the context of other enzyme systems that have provided evidence for hydrogen tunneling from the temperature dependence of isotope effects. These data emphasize the fundamental relationship between  $A_1/A_2$  and  $\Delta H^\ddagger$ .

**Table 1. Relationship among  $k_{\text{cat}}$ ,  $\Delta H^\ddagger$ , and KIE on Preexponential Arrhenius Factors**

enzyme	$\Delta H^\ddagger$ (kcal/mol) <sup>a</sup>	$A_D/A_T$
BSAO <sup>20</sup>	15.8	0.51
MAO-B <sup>24</sup>	15.0	0.52
GO <sup>30</sup>	11.0	1.3
SBL <sup>39</sup>	1.8	5.6 <sup>b</sup>

<sup>a</sup> For C–D bond cleavage. <sup>b</sup> Calculated from  $\ln(A_H/A_D)/\ln(A_D/A_T) = 2.26$ .

SBL KIEs were measured with either perdeuterated substrate or substrate that was dideuterated at the reactive, C11 position. This raised the possibility of a highly anomalous secondary kinetic isotope effect as the origin of a primary H/D KIE close to 60. This possibility has been ruled out by recent experiments using [11, S-<sup>2</sup>H]linoleic acid which indicate a similar, nearly temperature-independent primary H/D KIE.<sup>39</sup>

Two recent theoretical works have attempted to deal with this system. Antoniou and Schwartz<sup>26</sup> point out that a close to temperature-independent reaction rate and KIE will occur if  $V_p \approx -\epsilon$  (cf. Figure 7). This is a general situation in Marcus-like models going from normal to inverted regions.<sup>2,4</sup> Moiseyev, Rucker, and Glickman<sup>40</sup> present a dissipative tunneling method where the double well is static and the coherency is relaxed by fast electron transfer from the product well. This was accomplished using the formulation of Bethe.<sup>41</sup> The lower limit for the H/D KIE calculated by this model is  $2 \times 10^5$  while the experimental value is *ca.* 60. Trying to overcome this result, a very tight transition state (TS) was proposed. Specifically, the vibrational modes orthogonal to the reaction coordinate were proposed to have a much higher frequency at the TS than the ground state, such that an *inverse KIE* on the energy of activation results ( $E_a^H > E_a^D$ ). If large enough, this effect can compensate for the very large KIE arising from pure quantum mechanical effects, as the protium would tunnel through a higher barrier than deuterium. This phenomenon requires strong interactions between the transferred hydrogen radical and atoms geometrically close to its C → O path (strong meaning relative to the  $\sim 3000 \text{ cm}^{-1}$  C–H ground-state stretching vibration lost at the TS). By examining the available crystal structures of SBL (in the inactive, Fe(II) form) with docked substrate, no functional groups are apparent that could lead to such an interaction.<sup>42</sup> Although Moiseyev et al.<sup>40</sup> assumed  $\Delta H^\ddagger = 0$ , there is, in fact, a finite energy of activation on the C–H bond cleavage step of SBL. Thus, a more realistic model may involve dissipative tunneling via coupling to protein dynamics.

## Other Systems and Models

In addition to the examples mentioned above, evidence for proton tunneling and coupled motion was recently found experimentally in the triosephosphate isomerase reaction.<sup>43</sup> In addition to the theoretical methods mentioned, many other different models have been developed to test the importance of quantum mechanical effects in enzymatic systems such as serine proteases,<sup>44</sup> lactate dehydrogenase,<sup>45</sup> and carbonic anhydrase.<sup>46</sup> The conclu-

sion of the last authors was that although tunneling is extensive in the enzymatic reaction, it is also important in the solution reaction so that its contribution to catalysis is small but nonnegligible.<sup>46</sup> How unique is hydrogen tunneling to enzymatic systems? At low temperature, many solid-state reactions exhibit evidence for tunneling similar to that discussed above. At room temperature, a few reactions in organic solution exhibit behavior characteristic of tunneling such as H/D KIEs of 30–50 and values for  $A_H/A_T$  of 6–50.<sup>47–49</sup> Unlike SBL, however, these systems have a significant enthalpy of activation (5–15 kcal/mol) which would place them between systems III and IV of Figure 5.

## Conclusions

Since analytical or *ab initio* calculations are inapplicable for systems as large as enzymes in solution, the degree of tunneling in question is obviously model dependent. An interactive process, where models lead to predictions tested by experiments which lead to a new model, is what makes such research fruitful and exciting. Obviously, close collaboration between experimentalists and theoreticians is essential (though the lack of common language is often the rate-limiting step).

More than 10 enzymes and mutants mentioned above have demonstrated a behavior that cannot be explained without invoking hydrogen tunneling. We believe that a critical amount of evidence has accumulated, suggesting that hydrogen tunneling, under physiological conditions, is a generally important feature in enzyme-catalyzed reactions. Enzymes, which catalyze different reactions, via different mechanisms and accompanying charge transfer ( $H^+$ ;  $H^\bullet$ ;  $H^-$ ), appear to utilize tunneling.

Nuclear tunneling adds new features to the conventional view of enzyme catalysis. First, not only the thermodynamic height of the barrier (as in the conventional theory), but also its width, as well as the symmetry of the reactant and product potential surfaces, becomes an important factor for optimal catalysis. Second, classical models assume that all degrees of freedom which are orthogonal to the reaction coordinate are in equilibrium at the TS, whereas most tunneling models that go beyond an empirical correction to TST invoke potential surface dynamics which directly affect the reaction rate.

Is hydrogen tunneling under physiological conditions a unique feature of biocatalysis or is it of similar importance in noncatalyzed reactions? This question is still a controversial one, as good noncatalyzed reference reactions are hard to find. The data from this laboratory suggest that enzymes have evolved to impose critically controlled active site structures and dynamics to enhance tunneling. The degree of tunneling in each case is expected to be related to the ease (or difficulty) of invoking classical components to enhance the rate. The generality of these conclusions to other biological hydrogen (and possibly other nuclei) transfer processes remains to be examined. We believe that such a possibility should not *a priori* be excluded for any system which offers a well-

organized dynamic environment that can control donor–acceptor distance and orientation.

*J.P.K. acknowledges support from the NSF (Grant MCB-9514126) and the NIH (Grant GM25765).*

## References

- (1) Fersht, A. *Enzyme Structure and Mechanism*, 2nd ed.; W. H. Freeman: New York, 1985.
- (2) Marcus, R. A.; Sutin, N. *Biochim. Biophys. Acta* **1985**, *811*, 265–322.
- (3) Bell, R. P. *The Tunneling Effect in Chemistry*; Chapman & Hall: London and New York, 1980.
- (4) Melander, L.; Saunders: W. H. *Reaction Rates of Isotopic Molecules*; Krieger, R. E., FL, 1987.
- (5) Saunders: W. H. *J. Am. Chem. Soc.* **1985**, *107*, 164–169.
- (6) Grant, K. L.; Klinman, J. P. *Bioorg. Chem.* **1992**, *20*, 1–7.
- (7) Kim, T.; Kreevoy, M. M. *J. Am. Chem. Soc.* **1992**, *114*, 7116–7123.
- (8) Jonsson, T.; Glickman, M. H.; Sun, S.; Klinman, J. P. *J. Am. Chem. Soc.* **1996**, *118*, 10319–10320.
- (9) Cha, Y.; Murray, C. J.; Klinman, J. P. *Science* **1989**, *243*, 1325–1330.
- (10) Huskey, W. P.; Schowen, R. L. *J. Am. Chem. Soc.* **1983**, *105*, 5704.
- (11) Northrop, D. B. Determining the Absolute Magnitude of Hydrogen Isotope Effects. In *Isotope effects on Enzyme-Catalyzed Reactions*; Cleland, W. W., O’Leary, M. H., Northrop, D. B., Eds.; University Park Press: Baltimore, MD, 1977; p 122.
- (12) Bahnson, B. J.; Klinman, J. P. *Methods Enzymol.* **1995**, *249*, 373–397.
- (13) Rucker, J.; Cha, Y.; Jonsson, T.; Grant, K. L.; Klinman, J. P. *Biochemistry* **1992**, *31*, 11489–11499.
- (14) Bahnson, B. J.; Park, D.; Kim, K.; Plapp, B. V.; Klinman, J. P. *Biochemistry* **1993**, *32*, 5503–5507.
- (15) Bahnson, B. J.; Colby, T. D.; Chin, K. J.; Goldstein, B. M.; Klinman, J. P. *Proc. Natl. Acad. Sci. U.S.A.* **1997**, *94*, 12797–12802.
- (16) Kohen, A.; Cannino, R.; Bartolucci, S.; Klinman, J. P. Unpublished data, 1997.
- (17) Truhlar, D. G.; Gordon, M. S. *Science* **1990**, *249*, 491–498.
- (18) Klinman, J. P. *Chem. Rev.* **1996**, *96*, 2541–2561.
- (19) Palcic, M. M.; Klinman, J. P. *Biochemistry* **1983**, *22*, 5957–5966.
- (20) Grant, K. L.; Klinman, J. P. *Biochemistry* **1989**, *28*, 6597–6605.
- (21) Schneider, M. E.; Stern, M. J. *J. Am. Chem. Soc.* **1972**, *94*, 1517–1522.
- (22) Thibblin, A. *J. Phys. Org. Chem.* **1988**, *1*, 161–167.
- (23) Koch, H. F.; Dahlberg, D. B. *J. Am. Chem. Soc.* **1980**, *102*, 6102–6107.
- (24) Jonsson, T.; Edmondson, D. E.; Klinman, J. P. *Biochemistry* **1994**, *33*, 14871–14878.
- (25) Bruno, W. J.; Bialek, W. *Biophys. J.* **1992**, *63*, 689–699.
- (26) Antoniou, D.; Schwartz, S. D. *Proc. Natl. Acad. Sci. U.S.A.* **1997**, *94*, 12360–12365.
- (27) Borgis, D.; Hynes, J. T. *J. Chem. Phys.* **1991**, *94*, 3619–3628.
- (28) Weibl, M. K.; Bright, H. J. *J. Biol. Chem.* **1971**, *246*, 2734–2744.
- (29) Bright, H. J.; Appleby, M. *J. Biol. Chem.* **1969**, *244*, 3625–3634.
- (30) Kohen, A.; Jonsson, T.; Klinman, J. P. *Biochemistry* **1997**, *36*, 2603–2611.
- (31) Frederick, K. R.; Tung, J.; Emerick, R. S.; Masiarz, E. F.; Chamberlain, S. H.; Vasavada, A.; Rosenberg, S.; Chakraborty, S.; Schopfer, L. M.; Massey, V. *J. Biol. Chem.* **1990**, *265*, 3793–3802.
- (32) Rudd, P. M.; Joao, H. C.; Coghill, E.; Fiten, P.; Saunders: M. R.; Opdenakker, G.; Dwek, R. A. *Biochemistry* **1994**, *33*, 17–22.
- (33) Stubbe, J. A. *Annu. Rev. Biochem.* **1989**, *58*, 257–285.
- (34) Wiseman, J. S. *Biochemistry* **1989**, *28*, 2106–2111.
- (35) Glickman, M. H.; Klinman, J. P. *Biochemistry* **1996**, *35*, 12882–12892.
- (36) Glickman, M. H.; Klinman, J. P. *Biochemistry* **1995**, *34*, 14077–14092.
- (37) Glickman, M. H.; Wiseman, J.; Klinman, J. P. *J. Am. Chem. Soc.* **1994**, *116*, 793–794.
- (38) Hwang, C. C.; Grissom, C. B. *J. Am. Chem. Soc.* **1994**, *116*, 795–796.
- (39) Rickert, K.; Klinman, J. P. Unpublished results, 1997.
- (40) Moiseyev, N.; Rucker, J.; Glickman, M. H. *J. Am. Chem. Soc.* **1997**, *119*, 3853–3860.
- (41) Bethe, H. A. *Handb. Phys.* **1933**, *24/1*, 452.
- (42) Scarrow, R.; Rickert, K.; Klinman, J. P. Unpublished results, 1997.
- (43) Alston, W. C.; Maska, M.; Murray, C. J. *Biochemistry* **1996**, *35*, 12873–12881.
- (44) Sumi, H.; Ulstrup, J. *Biochim. Biophys. Acta* **1988**, *955*, 26–42.
- (45) Hwang, J. K.; Chu, Z. T.; Yadav, A.; Warshel, A. *J. Phys. Chem.* **1991**, *95*, 8445–8448.
- (46) Hwang, J. K.; Warshel, A. *J. Am. Chem. Soc.* **1996**, *118*, 11745–11751.
- (47) Caldin, E. F. *Chem. Rev.* **1969**, *69*, 135–156.
- (48) Kresge, A. J.; Powel, M. F. *J. Am. Chem. Soc.* **1981**, *103*, 201–202.
- (49) Roecker, L.; Meyer, T. J. *J. Am. Chem. Soc.* **1987**, *109*, 746–754.

AR9701225